Terahertz pulsed imaging of frozen biological tissues

Hiromichi Hoshina,[1,a)] Aya Hayashi,[1] Norio Miyoshi,[2] Fumiaki Miyamaru,[3,4] and Chiko Otani[1]
[1]*RIKEN, 519-1399 Aramaki-Aoba, Aoba-ku, Sendai, Miyagi 980-0845, Japan*
[2]*University of Fukui, Shimoaizuki, 23-3, Matsuoka, Yoshida-gun, Fukui 910-1193, Japan*
[3]*Department of Physics, Faculty of Science, Shinshu University, 3-1-1 Asahi, Matsumoto, Nagano 390-8621, Japan*
[4]*PRESTO, Japan Science and Technology Agency, 2-1-1 Katahira, Aobaku-ku, Sendai 980-8577, Japan*

(Received 30 October 2008; accepted 5 March 2009; published online 23 March 2009)

Recently, terahertz wave imaging has been shown to have potential in medical and biological applications. However, absorption by liquid water in tissues hinders the measurement of thick samples. In this study, porcine tissue was frozen to temperatures below −33 °C to prevent this absorption. Consequently, the striated muscle and adipose tissue could be clearly distinguished in the terahertz time-domain spectra owing to the difference in absorbance values and refractive indices. We demonstrated two-dimensional map of absorbance and terahertz pulse delay, which clearly shows the spatial distribution of the tissues. © *2009 American Institute of Physics*. [DOI: 10.1063/1.3106616]

With the development of technology for generating and detecting terahertz waves, various applications have been proposed in the past decade. The penetrability and appropriate spatial resolution of terahertz radiation enables perspective imaging, and the fingerprint spectra in this frequency region can be used for chemical identification.[1] This technology has useful applications for imaging in the medical field since different tissues have different optical properties, such as absorbance, refractive index, and reflectance.[2–6] Several studies have proposed the use of terahertz-wave imaging for observing skin burns[7] and dental tissue[8,9] and detecting skin cancer,[10–13] liver cancer,[14–16] and breast tumor.[17] However, the water in the tissues hinders observation by this method. Water strongly absorbs terahertz radiation (as much as ~300–1000 dB/cm),[2] allowing only a very weak terahertz transmission signal.[6] Only reflection-type imaging techniques succeed in observing tumors *in vivo* at the surface of the skin.[13]

In this study, the sample was frozen and the terahertz transmission spectra could be measured without absorption of radiation by liquid water. Sliced porcine tissue (available commercially as pork loin meat) was used as a sample; the striated muscle and the adipose tissue were clearly seen as red and white regions, as shown in Fig. 1. The tissue was cut into slices having a thickness of about 1.7 mm, which were sandwiched by a pair of 2-mm-thick quartz windows. The windows were attached to a copper cell and cooled to −33 °C by the circulation of a coolant, and the temperature of the cell was monitored using a thermocouple. The cell was installed at the focal point of a commercial terahertz time-domain spectrometer (TDS) (Aispec: pulse IRS-2300). The position of the cell was moved by a two-axis mechanical stage and two-dimensional spectroscopic images were obtained. The spot size of the terahertz beam was about 1 mm full width at half maximum at 1.0 THz. The optical path of the terahertz wave was purged by nitrogen gas in order to remove water vapor.

Figure 2 shows terahertz time-domain wave forms measured at 22 and −33 °C at points (a)–(e). The transmitted pulse is clearly seen in all of the tissues at −33 °C, while those at 22 °C are weaker due to the absorption of the radiation by water. Figure 3 shows the refractive indices and absorbance calculated using the wave forms shown in Fig. 2. Taking into account the Fresnel reflection at the interface between the sample and the windows, the complex refractive indices of the sample $\tilde{n}=n-i\kappa$ was calculated by using the following equations:

$$n(\omega)=\frac{c}{\omega d}\left\{\phi(\omega)+\arg\left\{\frac{\tilde{n}(\omega)[\tilde{n}_q(\omega)+1]^2}{[\tilde{n}_q(\omega)+\tilde{n}(\omega)]^2}\right\}\right\}+1, \quad (1)$$

$$\kappa(\omega)=-\frac{c}{\omega d}\ln\left\{\left|\frac{\tilde{n}(\omega)[\tilde{n}_q(\omega)+1]^2}{[\tilde{n}_q(\omega)+\tilde{n}(\omega)]^2}\right|\sqrt{T(\omega)}\right\}, \quad (2)$$

where $T(\omega)$ and $\phi(\omega)$ are the power transmittance and the phase difference between Fourier transformed spectra of the sample and the reference d is the thickness of the sample $\tilde{n}_q$ is the previously measured complex refractive index of quartz. Since these equations cannot be solved for n and κ, the values were calculated numerically, i.e., starting from

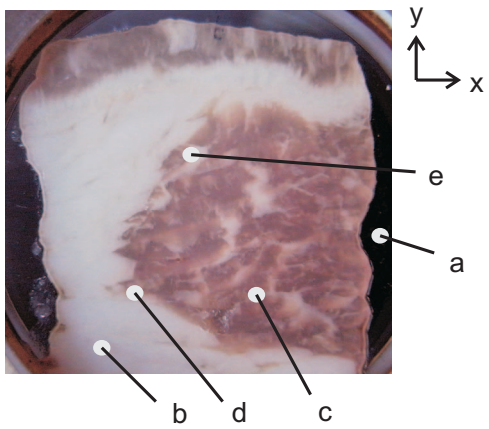

FIG. 1. (Color) Photographs of the porcine tissues in the sample cell.

a)Electronic mail: hoshina@riken.jp.

 © 2009 American Institute of Physics

Downloaded 25 Mar 2009 to 134.160.214.108. Redistribution subject to AIP license or copyright; see http://apl.aip.org/apl/copyright.jsp

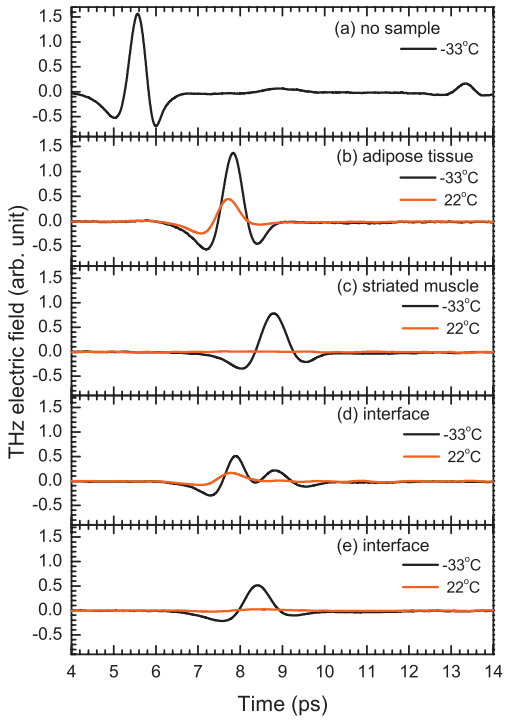

FIG. 2. (Color) Terahertz time-domain wave forms of the porcine tissue measured at 22 and −33 °C. The positions of traces [(a)–(e)] are specified in Fig. 1.

roughly estimated values of n and κ, the solutions of the equations were calculated iteratively until self-consistent results were obtained.[18] The thickness d of the sample was estimated to be 1.2 mm from the distance between main pulse peak and the second peak in trace (a); the second peak is due to the Fresnel reflection of the quartz window. The absorbance α was obtained by using the following equation:

$$\alpha(\omega) = \frac{2\omega\kappa(\omega)}{c}\log_{10} e.$$

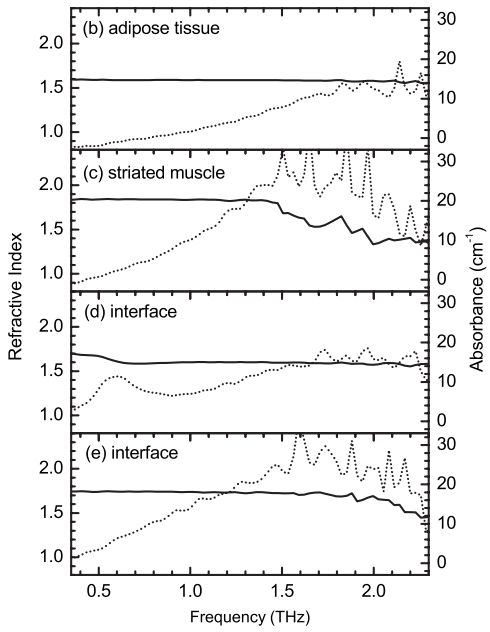

FIG. 3. Refractive index (solid line) and absorbance (dashed line) of the porcine tissue measured at −33 °C. The positions of traces [(b)–(d)] are the same as Fig. 2.

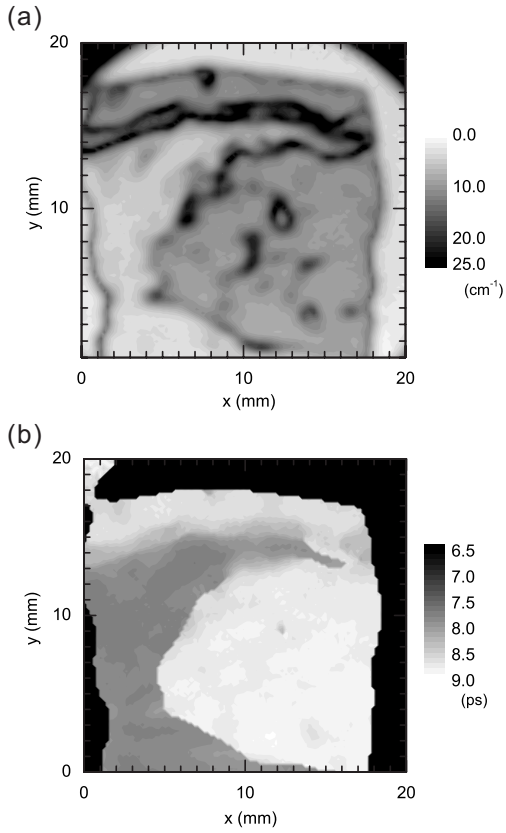

FIG. 4. Two-dimensional map of the absorbance at 1.0 THz (a) and the maximum peak position in the time-domain data (b).

The absorbance values of the adipose tissue and striated muscle increased continuously and reached the lower limit of the dynamic range of terahertz-TDS around 2.0 at 1.5 THz, respectively.[19] As in the case of the spectra of human tissues measured at the normal temperature, both the above spectra showed no characteristic peaks, and the absorbance of the striated muscle was 2.5–3.0 times higher than that of the adipose tissue. The refractive indices of the tissues are about 1.6 and 1.8, respectively, which is in good agreement with those obtained for human tissues.[2]

Traces (d) and (e) in Figs. 2 and 3 were recorded from the interface region between the striated muscle and the adipose tissue. In these positions, the terahertz beam spot covered both tissues at the same time. When the terahertz pulse passed through the region where the interface plane was parallel to the terahertz propagation direction, two separate terahertz pulses were transmitted and superimposed in the time-domain data and showed double peaks, as seen in trace (d) of Fig. 2. On the other hand, when the interface was perpendicular to the propagation direction, the observed time-domain wave form showed a single pulse peak at an intermediate time delay, as seen in trace (e). When the interface was tilted, both these effects were observed simultaneously. These effects result in a drastic change in the shape of the Fourier-transform spectra. For example, the peak around 0.6 THz in trace (d) of Fig. 3 is due to the interference of the double pulse in the time-domain wave form.

Using the obtained spectra, the two-dimensional spectroscopic image of the sample was created. In the measurement, the cell was moved to a position 200 μm away and the imaging spectra for 100×100 pixels (20×20 mm^2) were recorded in 7 h. Figure 4(a) shows the two-dimensional plot

Downloaded 25 Mar 2009 to 134.160.214.108. Redistribution subject to AIP license or copyright; see http://apl.aip.org/apl/copyright.jsp

of the absorbance at 1.0 THz. The small spots of adipose tissue distributed in the striated muscle appear in good contrast as dark areas. However, this contrast does not reflect the difference in the absorbance but the decrease in the terahertz pulse intensity at the interface of different kind of tissues. To overcome this problem and achieve a clear distinction between tissues, the position of the peak maximum in the terahertz time-domain wave form was used for the mapping showed in Fig. 4(b). Since the terahertz peak position at the interface lay between those of the two tissues, the position of the peak maximum changed continuously. Therefore, the effect of the multiple pulses at the interface was not strong and the tissues could be clearly distinguished. On the other hand, the small spots of the adipose tissues in the striated muscle were not clearly visible.

The authors would like to thank Dr. Yukihiro Fukunaga for his kind advice for this article. This work was supported in part by the Foundation for Promotion of Cancer Research in Japan. Fumiaki Miyamaru is also supported by Konica Minolta Co. Ltd.

[1]Y.-S. Lee, *Principles of Terahertz Science and Technology* (Springer, New York, 2009).
[2]A. J. Fitzgerald, E. Berry, N. N. Zinov'ev, S. Homer-Vanniasinkam, R. E. Miles, J. M. Chamberlain, and M. A. Smith, J. Biol. Phys. **29**, 123 (2003).
[3]S. M. Kim, F. Hatami, J. S. Harris, A. W. Kurian, J. Ford, D. King, G. Scalari, M. Giovannini, N. Hoyler, J. Faist, and G. Harris, Appl. Phys. Lett. **88**, 153903 (2006).
[4]J. Darmo, V. Tamosiunas, G. Fasching, J. Kröll, K. Unterrainer, M. Beck, M. Giovannini, J. Faist, C. Kremser, and P. Debbage, Opt. Express **12**, 1879 (2004).
[5]T. Löffler, K. Siebert, S. Czasch, T. Bauer, and H. G. Roskos, Phys. Med. Biol. **47**, 3847 (2002).
[6]T. Loffler, T. Bauer, K. J. Siebert, H. G. Roskos, A. Fitzgerald, and S. Czasch, Opt. Express **9**, 616 (2001).
[7]Z. D. Taylor, R. S. Singh, M. O. Culjat, J. Y. Suen, W. S. Grundfest, H. Lee, and E. R. Brown, Opt. Lett. **33**, 1258 (2008).
[8]E. Pickwell, V. P. Wallace, B. E. Cole, S. Ali, C. Longbottom, R. J. M. Lynch, and M. Pepper, Caries Res. **41**, 49 (2007).
[9]D. Crawley, C. Longbottom, V. P. Wallace, B. Cole, D. Arnone, and M. Pepper, J. Biomed. Opt. **8**, 303 (2003).
[10]R. M. Woodward, B. E. Cole, V. P. Wallace, R. J. Pye, D. D. Arnone, E. H. Linfield, and M. Pepper, Phys. Med. Biol. **47**, 3853 (2002).
[11]R. M. Woodward, V. P. Wallace, D. D. Arnone, E. H. Linfield, and M. Pepper, J. Biol. Phys. **29**, 257 (2003).
[12]R. M. Woodward, V. P. Wallace, R. J. Pye, B. E. Cole, D. D. Arnone, E. H. Linfield, and M. Pepper, J. Invest. Dermatol. **120**, 72 (2003).
[13]V. P. Wallace, A. J. Fitzgerald, S. Shankar, N. Flanagan, R. Pye, J. Cluff, and D. D. Arnone, Br. J. Dermatol. **151**, 424 (2004).
[14]J. Nishizawa, T. Sasaki, K. Suto, T. Yamada, T. Tanabe, T. Tanno, T. Sawai, and Y. Miura, Opt. Commun. **244**, 469 (2005).
[15]S. Nakajima, H. Hoshina, M. Yamashita, C. Otani, and N. Miyoshi, Appl. Phys. Lett. **90**, 041102 (2007).
[16]P. Knobloch, C. Schildknecht, T. Kleine-Ostmann, M. Koch, S. Hoffmann, M. Hofmann, E. Rehberg, M. Sperling, K. Donhuijsen, G. Hein, and K. Pierz, Phys. Med. Biol. **47**, 3875 (2002).
[17]A. J. Fitzgerald, V. P. Wallace, M. Jimenez-Linan, L. Bobrow, R. J. Pye, A. D. Purushotham, and D. D. Arnone, Radiology **239**, 533 (2006).
[18]M. Hangyo, T. Nagashima, and S. Nashima, Meas. Sci. Technol. **13**, 1727 (2002).
[19]P. U. Jepsen and B. M. Fischer, Opt. Express **30**, 29 (2005).

Downloaded 25 Mar 2009 to 134.160.214.108. Redistribution subject to AIP license or copyright; see http://apl.aip.org/apl/copyright.jsp